

4. V. E. Chekalin and Yu. I. Chistov, "Experimental investigation of heat transfer in a conical supersonic nozzle," Tr. TsAGI, No. 1146 (1969).
5. N. I. Khvostov, A. D. Sukhobokov, V. E. Chekalin, and K. N. Skirda, Inzh.-Fiz. Zh., 29, No. 1 (1975).
6. M. D. Zdunkevich, R. M. Sevast'yanov, and N. A. Zykov, Tr. TsAGI, No. 1165 (1969).
7. N. J. Khvostov, NASA CR-2569, Appendix C (July, 1975).
8. T. A. Timofeeva and Yu. I. Chistov, Tr. TsAGI, No. 1403 (1972).
9. N. B. Vargaftik, Tables on the Thermophysical Properties of Liquids and Gases, Halsted Press (1975).

FLOW OF VISCOUS INCOMPRESSIBLE LIQUID IN A PLANE CHANNEL WITH ABRUPT ONE-SIDED BROADENING

V. I. Korobko, É. M. Malaya,
and V. K. Shashmin

UDC 532.516.5

A numerical solution is obtained for the Navier—Stokes equations in the problem of laminar flow of a viscous incompressible liquid in a plane channel with abrupt one-sided broadening. The solution is compared with experiment.

The flow of a viscous incompressible liquid in a channel with abrupt broadening is of great practical interest. Such flows are investigated on the basis of the complete Navier—Stokes equations, since viscosity effects play a large role. Abrupt broadening of the channel is associated with breakaway of the flow from the wall and the formation of a region of return flow.

The laminar flow of viscous incompressible liquid in channels with abrupt broadening has been studied both numerically and experimentally. In [1], numerical calculations were made of the flow in an abruptly broadening and abruptly narrowing channel, with displacement of one of its walls, at Reynolds numbers $Re \leq 1000$, and the dependence of the breakaway-region length on Re was obtained for a given broadening. In [2] the periodic flow in a channel with abrupt broadening was investigated numerically for $Re \leq 200$. The difficulty in experimental investigations of such flows is to measure the velocities in the return-flow region, which are very small. Electrothermoanemometers and laser anemometers are used for this purpose. In [3-5], the results of laminar-flow-velocity measurements in channels were given, and in [6] the velocity field in the recirculation region was measured for abrupt broadening of the channel. In [7] the development of an unbounded flow along a wall with a step was investigated; the effect of the boundary-layer thickness at the step on the length of the recirculation region was found to be small [7]. In [8] the velocity field was measured for a laminar field of viscous incompressible liquid in a plane channel with one-sided broadening ($H/h_1 = 1.5$; $Re = u_0 h_1 / \nu = 146, 250, 382, 458$). The numerical results of [9] show that the recirculation region is longer than in [8], which is a consequence of the form of the initial velocity profile; this effect was not investigated experimentally. Analogous conclusions were reached in [10, 11] in an experimental investigation of the development of a flow of viscous incompressible liquid in channels with "ribs." In [12], the motion of an unbounded flow at a step was investigated numerically at $Re \geq 10^4$. Numerical calculation of the flow in a channel with a step [13] ($H/h_1 = 1.1$) showed that the length of the return-flow region is independent of Re ($25 \leq Re \leq 100$). In [14], the results of a numerical calculation of the flow in a channel with abrupt broadening ($H/h_1 = 8$) are given and, in particular, the dependence of the length of the return-flow region on Re ($Re \leq 120$) was obtained. In [15], an analogous investigation was made for $H/h_1 = 1.5$ and $Re \leq 40$. Numerical methods of solving Navier—Stokes equations for use with the given type of flow are reviewed in [16-18]. The present work gives the results of a numerical calculation of a laminar flow of viscous incompressible liquid in a channel with abrupt one-sided broadening ($H/h_1 = 3.2, 5.2, 6.2, 7.4, 8.2$). The calculation is made on the basis of the complete Navier—Stokes equations for $Re = 180$.

The system of Navier—Stokes equations describing the flow of viscous incompressible liquid in a plane channel is of the form [16]

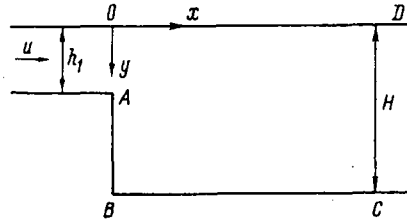


Fig. 1. Flow diagram.

$$\begin{aligned} \frac{\partial u}{\partial t} + u \frac{\partial u}{\partial x} + v \frac{\partial u}{\partial y} &= -\frac{\partial P}{\partial x} + \frac{1}{\text{Re}} \left(\frac{\partial^2 u}{\partial x^2} + \frac{\partial^2 u}{\partial y^2} \right), \\ \frac{\partial v}{\partial t} + u \frac{\partial v}{\partial x} + v \frac{\partial v}{\partial y} &= -\frac{\partial P}{\partial y} + \frac{1}{\text{Re}} \left(\frac{\partial^2 v}{\partial x^2} + \frac{\partial^2 v}{\partial y^2} \right), \\ \frac{\partial u}{\partial x} + \frac{\partial v}{\partial y} &= 0. \end{aligned} \quad (1)$$

Introducing the current function ψ and the vorticity ξ [16]

$$u = \partial\psi/\partial y, \quad v = -\partial\psi/\partial x; \quad \xi = \nabla^2\psi, \quad (2)$$

these equations reduce to a system of two equations in (ψ, ξ) , which are written in divergent form [18]

$$\frac{\partial \xi}{\partial t} = \frac{1}{\text{Re}} \nabla^2 \xi - \frac{\partial}{\partial x} (\xi u) - \frac{\partial}{\partial y} (\xi v), \quad \xi = \nabla^2 \psi. \quad (3)$$

Writing finite differences for Eq. (3) leads to a system of finite-difference equations in conservation-law form [19].

The present work uses an explicit two-layer difference scheme of second-order accuracy with a one-sided approximation of the convection terms. The diffusion terms in Eq. (3) are written using central differences. In terms of convective transfer, information passes into a cell only from cells that lie upstream from it [20], and therefore the convective terms are written using differences in the upstream direction with an accuracy of $O(h^2)$. When the sign of the velocity changes close to the nodal point, it is necessary to change the form of the basic scheme, according to which differences are written in the upstream direction. At a distance of one spatial step from the boundary of the region, a central-difference approximation is used for the convective terms. The Laplace operator in Eq. (3) is approximated by central differences. Thus, Eq. (3) is approximated by a finite-difference system with an error of $O(\Delta t + h^2)$.

The stability of the resulting finite-difference system in (ψ, ξ) was analyzed by the Neumann method [17]. The stability condition for the given system was taken in the form: $\Delta t \leq a \Delta x^2$, where a is some constant of order 1/2.

In solving the finite-difference system, it is necessary to formulate boundary conditions for the vorticity ξ . These conditions may be obtained approximately using the values of the current function ψ already found. In [21] different means of specifying the boundary conditions for ξ are given.

The initial and boundary conditions for flow in a plane channel with abrupt one-sided broadening (Fig. 1) are

$$\begin{aligned} \psi &= 1, \quad \frac{\partial \psi}{\partial y} = 0, \quad \frac{\partial \psi}{\partial x} = 0 \quad \text{on } ABC, \\ \psi &= 0, \quad \frac{\partial \psi}{\partial y} = 0, \quad \frac{\partial \psi}{\partial x} = 0 \quad \text{on } OD, \\ \psi &= \int_0^y f(y) dy \quad \text{on } OA, \\ \frac{\partial \xi}{\partial x} &= 0, \quad \frac{\partial \psi}{\partial x} = 0 \quad \text{on } DC, \\ \xi &= \frac{2(\psi_{w+1} - \psi_w)}{h^2} + f'(y) \quad \text{on } OA, \end{aligned} \quad (4)$$

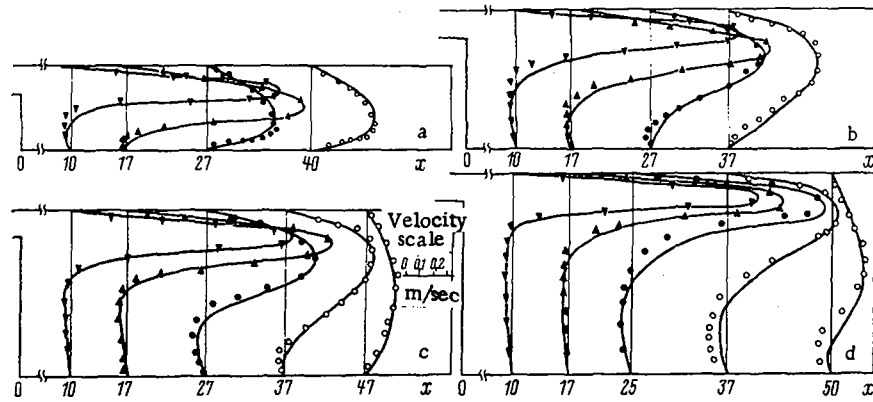


Fig. 2. Velocity profiles in a channel with one-sided broadening: the continuous lines show the results of calculation, while the points are experimental data; a) $H/h_1 = 3.2$; b) 5.2; c) 6.2; d) 7.4. x , mm.

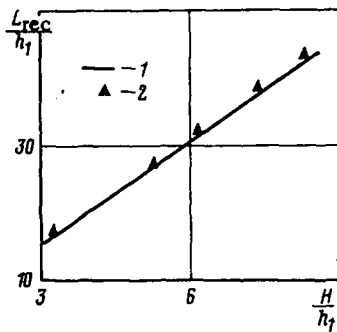


Fig. 3. Recirculation-region length as a function of the degree of channel broadening: 1) calculation by the scheme outlined; 2) experimental data.

$$\xi = \frac{8\psi_{w+1} - \psi_{w+2} - 7\psi_w}{2h^2} \text{ on } ABC \text{ and } OD, \quad (4)$$

where w is a boundary point, and $w + 1$ and $w + 2$ are adjacent boundary points; $f(y)$ is the given velocity distribution at the inlet. Note that the condition at the line DC in Eq. (4) corresponds to leveling out of the flow conditions far downstream. In the calculation, the condition at the line DC is taken at a finite distance from the step. The condition of DC is satisfied using a nonuniform grid in x , so as not to increase the number of grid points no matter how far away the condition at DC is taken. In [2] the Navier-Stokes equations were closed downstream using the boundary-layer equations. In [10], linear interpolation of the current function and the vorticity inside the flow region was used at the line DC.

The solution of the resulting finite-difference system of equations was obtained as follows. Suppose that at a certain time the grid functions $\psi_{i,j}^n$, $\xi_{i,j}^n$ are known. From the difference analog of the first relation in Eq. (3), it is then possible to find $\xi_{i,j}^{n+1}$ at the internal points of the grid region. Using the Zeidel' iterational method [21] to solve the difference analog of the second relation in Eq. (3) for the known boundary values of $\psi_{i,j}^{n+1}$ in Eq. (4), $\psi_{i,j}^{n+1}$ is found inside the region. From the values of $\psi_{i,j}^{n+1}$, the vortices $\xi_{i,j}^{n+1}$ at the boundary are found. Thus, values of $\psi_{i,j}^{n+1}$ and $\xi_{i,j}^{n+1}$ are obtained over the whole flow region. The calculation was carried out on an M-220M computer: the maximum number of points of the calculation grid was 1500; the accuracy of the Zeidel' iteration was 0.001; the grid step $\Delta x = \Delta y = h = 0.1$; and the time step $\Delta t = 0.01$. The printout gave the velocity profiles u , v at any cross sections of the channel, and the coordinate values of the current line $\psi = \psi_1 = \text{const}$ for $x = x_i$. At the end of the calculation, the fields of the current function ψ and the vorticity ξ were printed out.

A Diza-Élektronik thermoanemometric apparatus was used for an experimental investigation. The basic parameters of the apparatus and single-wire pickups used to measure the velocity field were as follows: wire diameter $d = 5 \mu$; wire length $l = 1.5$ mm; accuracy of the apparatus at low velocities (up to 4 m/sec), 0.2%. The velocity field was measured across the channel cross section for channel broadening characterized by the ratio

$H/h_1 = 3.2, 5.2, 6.2, 7.4,$ and 8.2 . The maximum velocity at the channel inlet was $u_m = 1.8$ m/sec. The Reynolds number $Re = u_m h_1 / \nu = 180$. The measurements showed that the velocity field at the channel outlet before broadening is described by the formula for laminar flow in a plane channel

$$\frac{u}{u_m} = 1 - 4 \frac{y^2}{h_1^2}.$$

Numerical and experimental velocity distributions in the channel are shown in Fig. 2 for $H/h_1 = 3.2, 5.2, 6.2,$ and 7.4 . The numerical calculations give a larger value of the rate at which the flow reaches perfectly developed laminar conditions after broadening than was observed experimentally. Since the condition at the line DC corresponds to the condition of flow-equalization at infinity, and this condition is imposed at a finite distance from the step, which must affect the more rapid equalization of the flow. In Fig. 3, the change in recirculation-region length is shown as a function of the degree of channel broadening. It is evident from Figs. 2 and 3 that the results of numerical calculation are in good agreement with the experimental data.

NOTATION

x, y , dimensionless coordinates referred to the characteristic length of the channel L (Fig. 1); $u, v, x,$ and y , components of the velocity, referred to the characteristic velocity u_0 ; P , dimensionless pressure; $Re = u_0 L / \nu$, Reynolds number, composed of the characteristic velocity u_0 , the characteristic length L , and the kinematic viscosity ν ; i, j , indices of the grid points over the x and y axes; n , iterational index; $\Delta x, \Delta y$, grid steps along the x and y axes; Δt , time step; u_m , maximum inlet velocity at channel axis; h_1, H , channel half-width at inlet and outlet (Fig. 1); ∇^2 , Laplace operator.

LITERATURE CITED

1. L. M. Simuni, "Numerical solution of some problems of viscous-liquid motion," *Inzh.-Fiz. Zh.*, 4, No. 3 (1964).
2. V. N. Varapaev, "Numerical investigation of periodic jet flow of viscous incompressible liquid," *Izv. Akad. Nauk SSSR, Mekh. Zhidk. Gaza*, No. 3 (1968).
3. R. J. Goldstein and D. K. Kried, *J. Appl. Mech.*, 34, 813 (1967).
4. N. S. Berman and V. A. Sontos, *A.I.Ch.E. J.*, 15, 323 (1969).
5. M. R. Samuels and D. M. Wetzal, *Chem. Eng. J.*, 4, 41 (1972).
6. F. Durst, A. Melling, and J. H. Whitelaw, in: *Proceedings of DISA Conference. Fluid Dynamic Measurements in the Industrial and Medical Environments, Leicester (1972)*, p. 81.
7. R. J. Goldstein, V. L. Friksen, R. M. Obson, and E. R. Ecket, *J. Bas. Eng.*, 92, 732 (1970).
8. M. K. Denham and M. A. Patrick, "Laminar flow over a downstream-facing step in a two-dimensional flow channel," *Trans. Inst. Chem. Eng.*, 52, No. 4 (1974).
9. D. J. Atkins, Ph. D. Thesis, University of Exeter (1974).
10. L. C. Leal and A. Acrivos, *J. Fluid Mech.*, 39, 735 (1969).
11. R. A. O'Leary and T. J. Mueller, Technical Report THEMISUND-69-4, College of Engineering, Notre Dame Univ. (1969).
12. P. J. Reache and T. J. Mueller, "Numerical solution of laminar separated flow," *AIAA J.*, 8, No. 3 (1970).
13. T. D. Taylor and E. Ndefo, "Calculation of viscous liquid flow in a channel by the separation method," in: *Numerical Methods in Fluid Mechanics [Russian translation]*, Mir, Moscow (1973).
14. G. F. Chavez and E. G. Richards, "A numerical study of the Coanda effect," *Pap. Am. Soc. Mech. Eng.*, No. Fles 12 (1970).
15. S. Uchida and M. Endo, "On some numerical solutions of the flow through a back-step channel," *Mem. Fac. Eng. Nagoua Univ.*, 27, No. 1 (1975).
16. I. Yu. Brailovskaya, T. V. Kuskova, and L. A. Chudov, "Difference methods of solving Navier-Stokes equations," in: *Computational Methods and Programing [in Russian]*, No. 11, Moscow State Univ. (1968).
17. R. Richtmeyer and K. W. Morton, *Difference Methods for Initial-Value Problems*, Interscience, New York (1967).
18. Cheng Sin-I, "A critical review of numerical solutions of Navier-Stokes equations," *Lect. Notes Phys.*, 41, 78-225 (1975).
19. P. D. Lax, "Weak solution of nonlinear hyperbolic equations and their numerical computation," *Commun. Pure Appl. Math.*, 7, 159-193 (1954).

20. R. Courant, E. Isaacson, and M. Rees, "On the solution of nonlinear hyperbolic difference equations by finite differences," *Commun. Pure Appl. Math.*, 5, No. 243 (1952).
21. R. P. Fedorenko, "Iterational methods of solving elliptical difference equations," *Usp. Mat. Nauk*, 28, No. 2 (170) (1973).

USING THE THEORY OF THE VOLUMETRIC FILLING OF
MICROPORES TO CALCULATE THE SORPTION OF
ELECTRICALLY INSULATING CELLULOSE MATERIALS

L. S. Kalinina and N. E. Gorobtsova

UDC 533.583.2

It is shown that the theory of the volumetric filling of micropores may be used to calculate sorption isotherms and the specific isothermal moisture capacity of electrically insulating cellulose materials.

In [1, 2] values of the equilibrium moisture content of electrically insulating cellulose materials were given for a wide range of sorption parameters — temperature and pressure. As noted in [1, 2], the sorption isotherms of cellulose materials for water-vapor pressures in the range of practical importance for the vacuum drying of electrical insulation ($P/P_S < 0.3$) are described by an equation of Freundlich type

$$W_e = cP^n, \quad (1)$$

where c and n are temperature-dependent constants characterizing the given material.

The sorption-isotherm equation of Freundlich type may be regarded as a particular case of the generalized absorption-isotherm equation for microporous sorbents based on the theory of volume filling, which in energy form, is written as follows [3-5]

$$w_e = W_0 \exp [-(A/E)^m], \quad (2)$$

where W_0 is a certain value of the adsorption, called the limiting value of the adsorption; A , differential work of adsorption ($A = RT \ln P_S/P$); E , characteristic adsorption energy determined at the characteristic point for a filling of $W_e/W_0 = \Theta = \exp(-1) = 0.368$; m , power index or the rank of the distribution. Together, m and E characterize the mechanism of the sorption interaction. When $m = 1$, Eq. (2) may be written in the Freundlich form in Eq. (1), and the empirical coefficients n and c in Eq. (1) are then [4]

$$n = RT/E, \quad (3)$$

$$c = W_0 P_S^{-n}. \quad (4)$$

Equation (2) provides a good description of the sorption equilibrium of various gases and vapors on microporous sorbents: active charcoals of various types, zeolites [3-5].

With a view to broadening the class of adsorbate-adsorbent systems for which the engineering method of equilibrium-adsorption proposed in [5] may be used, it is of interest to analyze experimental data on the equilibrium moisture content of electrically insulating cellulose materials. The interaction of water with these materials is a complex process whose mechanism is by no means fully understood, especially at low moisture contents. According to one viewpoint, the cellulose-water system should be regarded as the interaction of a polymer with the vapors of low-molecular solubility of water in cellulose [7]. Real cellulose systems — especially those which are electrically conducting — constitute complex fiber-porous systems, which may contain not only dissolved and adsorption-bound water, but also moisture bound by capillary and osmotic forces.

A. V. Lykov Institute of Heat and Mass Transfer, Academy of Sciences of the Belorussian SSR, Minsk. Translated from *Inzhenerno-Fizicheskii Zhurnal*, Vol. 35, No. 6, pp. 1084-1088, December, 1978. Original article submitted October 27, 1977.